Journal of Cerebral Blood Flow & Metabolism (2015) 35, 734–738

www.jcbfm.com

BRIEF COMMUNICATION

A mouse model of small-vessel disease that produces brain-wide-identified microocclusions and regionally selective neuronal injury

Gergely Silasi[1,2], Jennifer She[1], Jamie D Boyd[1,2], Songchao Xue[1] and Timothy H Murphy[1,2]

We developed a mouse model of small-vessel disease where occlusions are produced through endovascular injection of fluorescent microspheres that target ~12 μm diameter penetrating arterioles and can be localized in histology. Using Thy1-GFP transgenic mice, we visualized the impact of microocclusions on neuronal structure. Microocclusions in the hippocampus produce cell loss or neuronal atrophy (~7% of lodged microspheres led to microinfarcts), while axons within white matter tracts, as well as the striatum and thalamus became blebbed or disrupted. Although the neocortex contained more occlusions than other structures, labeled layer 5 neurons were relatively resistant to structural damage, with < 2% of the lodged microspheres producing obvious neuronal damage.

Journal of Cerebral Blood Flow & Metabolism (2015) **35,** 734–738; doi:10.1038/jcbfm.2015.8; published online 18 February 2015

Keywords: diffuse vascular injury; microinfarcts; mouse; stroke

INTRODUCTION

The need for reliable animal models of small-vessel disease is great, as the microinfarcts that produce this condition in humans are difficult to study in patient populations.[1] Elegant work in rats and mice disrupted flow in single vessels by targeting 10- to 20-μm-penetrating arterioles with laser light to produce either a thrombosis or a microhemorrhage in the cortex.[2,3] Although this work is informative, it involves manually targeting and occluding individual arterioles that are optically accessible. Other rodent models produce a shower of clots by injecting cholesterol-derived microcrystals ~100 μm in size through the carotid artery.[4–6] This shot-gun approach has the advantage of targeting a large number of vessels globally throughout the brain, thus modeling microinfarcts in humans. However, because the occluding crystals cannot be visualized during histologic analysis it is difficult to determine how many crystals actually lodge inside the brain. We chose to build on this approach by targeting small-penetrating arterioles by injecting ~20 μm fluorescent microspheres unilaterally through the common carotid artery of mice. This model allows us to conveniently identify blocked vessels by localizing the fluorescent beads in histologic sections, thus providing assessment of neuronal damage at sites with occlusions. We used this model in transgenic mice expressing green fluorescent protein (GFP) in a subpopulation of neurons to describe the impact of microocclusions on neuronal structure in multiple brain regions.

MATERIALS AND METHODS

Subjects and Experimental Design

Experiments were performed on male and female thymocyte differentiation antigen 1-GFP-m mice[7] that were 2 to 4 months old at the time of microsphere injection and were killed 8 to 10 days later. All surgical procedures were approved by the University of British Columbia Animal Care and Ethics Committee. Results were analyzed with a Kruskal–Wallis nonparametric one-way analysis of variance where ranking scales were used (histologic assessment and Neurologic Deficit Scale; see Supplementary Figure 1).

Surgical Procedure for Microsphere Injection

Fluorescent microspheres were injected unilaterally into the common carotid artery of mice to produce microocclusions by lodging in brain vessels (Figure 1A; see Supplementary Methods). The microsphere diameter of ~20 μm was selected to approximate the size of rodent penetrating arterioles that range from 10 to 20 μm.[8] To visualize the impairment in blood flow produced by the microspheres, mice were injected with Texas Red–conjugated dextran (70 kDa; Molecular Probes, Eugene, OR, USA) via the tail vein 1 hour before perfusion fixation. The majority of the dextran was thus cleared from vessels during the perfusion process, however blocked vessels typically retained dextran[9] in a segment around the lodged microspheres.

Sequential Dendritic/Axonal Analysis and Fluoro-Jade Staining

Histologic sections (150 μm) were mounted on slides and temporarily coverslipped with PBS as the mounting medium. After confocal images of structural damage in GFP-labeled cells were acquired, the coverslip was removed, and the slides progressed through the Fluoro-Jade (Histo-Chem, Jefferson, AR, USA) staining procedure. To completely quench the endogenous GFP signal the concentration of the $KMnO_4$ solution was increased to 0.25%.

[1]Department of Psychiatry, Kinsmen Laboratory of Neurological Research, Vancouver, British Columbia, Canada and [2]Brain Research Centre, University of British Columbia, Vancouver, British Columbia, Canada. Correspondence: Dr TH Murphy, 2255 Wesbrook Mall, Detwiller Pavilion Rm. 4N1, Vancouver, Canada B.C. V6T 1Z3.
E-mail: thmurphy@mail.ubc.ca
This work was supported by a Canadian Institutes of Health Research (CIHR) Operating Grant MOP-111009, a Heart and Stroke Foundation of Canada Grant in Aid, and a Canadian Partnership for Stroke Recovery expansion grant to THM. GS was supported by a CIHR postdoctoral fellowship and the Canadian Partnership for Stroke Recovery, and JS was supported by a scholarship from the Canadian Stroke Network.
Received 16 September 2014; revised 6 January 2015; accepted 7 January 2015; published online 18 February 2015

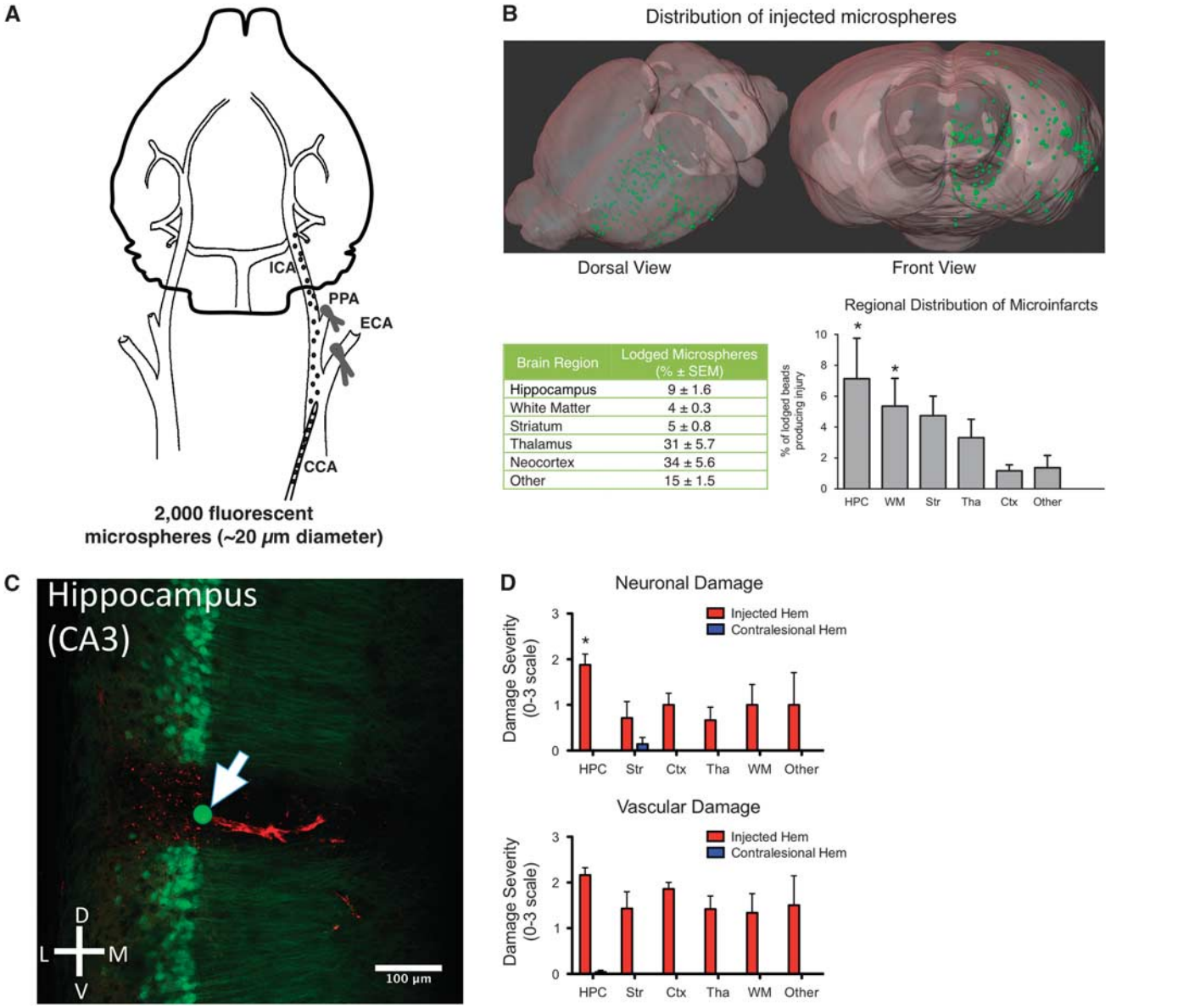

Figure 1. Fluorescent microspheres were injected into the common carotid artery (CCA) of mice, while the pterygopalatine (PPA) and external carotid arteries (ECA) were transiently blocked (**A**). The distribution of microspheres was visualized by reconstructing the brain from low-magnification images of 150 μm brain sections. For three-dimensional visualization, the fluorescent signal from microspheres was masked in Photoshop, and the stack of images was rendered in Amira (**B**, upper). Manual counting indicated that the majority of microspheres were lodged in the cortex or thalamus (~66% of total), however, the incidence of microinfarction was significantly greater in the hippocampus and white matter, compared with neocortex (**B**, lower). An example of microinfarction in the hippocampal CA3 field shows a microsphere (arrow) lodged in a vessel that has retained dextran (red) after perfusion fixation and the focal loss of CA3 neurons. The extravasation of dextran at the site of injury is also visible (**C**; red background signal). Quantification of neuronal damage showed significantly more severe injury in the hippocampus relative to the striatum, cortex, or thalamus (**D**, upper), while the severity of vascular damage did not differ among brain regions (**D**, lower).

RESULTS

Unilateral Trapping of Fluorescent Microspheres in Small Vessels

The distribution of microspheres was quantified by counting through an epifluorescent microscope. Each section was also imaged with a low-power objective (x2.5) and the distribution of the beads within the brain was reconstructed by assembling images of serial sections using Amira software (FEI, Hillsboro, OR, USA) (Figure 1B, upper; see Supplementary Movie). During manual counting, we found 423 ± 218 microspheres lodged in each brain, with the majority located in the cortex (34% ± 5.6%) or thalamus (31% ± 5.7%; Figure 1B). To further characterize the category of vessels blocked by the microspheres, we measured vessel diameter on either side of the microsphere in a mouse killed 4 hours after the surgery, before ischemic degradation of the vessel. The mean diameter for blocked vessels was 12.36 ± 0.5 μm in the cortex, 11.04 ± 0.2 μm in the striatum, and 10.26 ± 0.1 in the thalamus, consistent with measures of penetrating arteriole diameter *in vivo*,[3] however, it is likely that other vessel classes may also be blocked.

Incidence of Dendritic and Vascular Abnormalities because of Microocclusions Vary within Brain Regions

To quantify the distribution of microocclusions throughout the brain, the tissue around each lodged microsphere was imaged

using a confocal microscope and classified as either damaged or not. Damaged sites were ranked as either: (1) mild dendritic/axonal blebbing ($< 50\%$ of the 636 μm field of view); (2) severe dendritic/axonal blebbing ($> 50\%$ of the field of view) or presence of GFP-labeled puncta indicative of degraded neurons; or (3) loss of cell bodies or paucity of dendrites/axons. Damaged sites typically also had evidence of Texas Red–label accumulation within the blocked vessel or extravasation into the brain tissue (Figure 1C). Based on these criteria, we found that across the entire brain, 16.4% of the lodged microspheres produced identifiable damage to the neuronal structure. Dividing across brain regions, the percentage of microspheres producing damage in the hippocampus (7.1 ± 2.6; $P = 0.024$) or white matter (5.36 ± 1.8; $P = 0.05$) was significantly greater compared with the neocortex (1.17 ± 0.4, $n = 6$ mice). To further qualitatively assess the severity of each microocclusion, a masked observer ranked the severity of damage in both the GFP and Texas Red channels. To reduce experimenter bias, the microsphere in each image was masked with a black circle, and an identical black mask was placed in the homotopic cortex (same section) where there were no microspheres. The ranking scale for the GFP channel was the same as above, while the Texas Red channel was independently ranked 0 to 3 (0 = no damage; 1 = moderate extravasation; 2 = severe extravasation; and 3 = severe extravasation with distinct blocked vessel). Analyses showed significant neuronal ($P < 0.0001$) and vascular ($P < 0.0001$) damage in the injected hemisphere relative to homotopic areas ($n = 6$ mice; 465 sites examined). Comparing the severity of the damage across brain structures showed that the hippocampus had more severe neuronal damage compared with the cortex, striatum, or thalamus ($P < 0.032$; Figure 1D, upper). Although the severity of vascular damage did not differ among brain structures ($P = 0.146$; Figure 1D, lower), there was a significant correlation between vascular and neuronal damage (Spearman's $\rho = 0.694$, $P < 0.001$). Damaged sites in the Cornu Ammonis fields of the hippocampus were typically characterized by a focal loss of cell bodies forming a wedge-shaped lesion spanning 100 to 400 μm in diameter (Figure 2A). In our 150-μm thick sections, lesions caused by a single blocked vessel often extended through several sections (Figure 2A). Other hippocampal structures such as the hilus, dentate gyrus, and fornix also had clear damage in some animals. Damaged white matter tracts (corticofugal fibers in the striatum, corpus callosum, cerebral peduncles, and anterior commissures; Figure 2B) were characterized by blebbing or a focal loss of GFP label within a well-defined tract. Similar damage to white matter tracts has been reported after endothelin-1 injection into the corpus callosum[10] and chronic hypoperfusion in a mouse model of vascular cognitive impairment.[11] Cortical damage when present included blebbed axonal/dendritic processes and an absence of cell bodies in severe cases (Figure 2C).

Coincidence of Markers of Cell Death, Microglial Activation, and Dendritic Damage after Microinfarction

In a subset of animals ($n = 5$ microinfarct mice; $n = 4$ sham), we performed sequential imaging of structural damage in GFP-labeled cells and Fluoro-Jade staining to directly identify damaged neurons at an 8-day survival. Most of the focal lesions identified by imaging of endogenous GFP also contained Fluoro-Jade-positive cells indicating neuronal degeneration (Figure 2A), while other (less severely) injured sites were devoid of Fluoro-Jade label. Our observation that only a subset of the occlusions produce ischemic injury was further confirmed by our observation that microglial activation was only present at 21% of occlusion sites (440 microspheres examined; $n = 3$ mice; Supplementary Figure 2). In sum, these results show that the incidence of ischemic injury, quantified as either local neuronal damage in Thy1-GFP mice, or microglial activation, is approximately equal in this model (16% versus 21% incidence, respectively).

DISCUSSION

Producing Microocclusions Through Unilateral Microsphere Injection allows for Quantification of Dendritic/Axonal Injury and Neuronal Death Throughout Entire Mouse Brain

Previous methods for producing a shower of clots within the rodent brain relied mostly on cholesterol crystals,[6] and used immunohistochemical markers of damage to indirectly identify sites where vessels were blocked. In one study, fluorescent microspheres were injected intraarterially in rats, and the amount of recovered fluorescence in homogenized brain samples was quantified to indicate incidence of trapped microspheres.[12] Our current study built on these methods by developing a protocol for directly quantifying the distribution of lodged microspheres within the mouse brain, visualizing the local impairment in blood flow with dextran trapped in blood vessels, and quantifying neuronal damage in the form of cell death and dendritic/axonal injury. By using transgenic mice expressing GFP in a subset of neurons (Thy1-GFP), we did not need to perform additional labeling to visualize neurons and their processes such as Golgi labeling that would preclude the use of other fluorescent reagents. However, it is possible that using a pan-neuronal marker would have revealed focal neuronal damage at locations where only fibers of passage were labeled in our animals. Conveniently, we were able to complement our imaging of GFP expression in neurons with a modified Fluoro-Jade procedure, as well as a quantification of the microglial response to injury. Fluoro-Jade labeling confirmed that identified microocclusions contained degenerating neurons, while microglial labeling showed that such injury also produces an inflammatory glial response similar to microinfarcts in humans.[3] Overall, the structural damage produced in this model shares features with the disruption in connectivity seen in patients with small vessel disease.[13]

Incidence of Microinfarction after Microsphere Injection Varies Across Brain Regions

Similar to previous findings,[6,12,14] our data show that the majority of lodged microspheres do not cause microinfarction as only 16% of the microspheres produced detectable neuronal structural damage, and 21% triggered microglial activation. Reactive gliosis often coincides with microglial activity in microocclusions,[6] however, we did not evaluate this here. We report that the distribution of lodged microspheres within the brain is not random, as there is greater accumulation of microspheres in the cortex and thalamus than would be expected based on the volume of these structures. For example, the thalamus and striatum are similar in volume, but the thalamus accumulated six times more microspheres. One possible explanation is that microsphere distribution is influenced by the level of vascularization of each brain structure. Relative to the cortex, the hippocampus and white matter have lower capillary densities in mice.[15] In our experiments, these same structures accumulated fewer lodged beads, but were more susceptible to microocclusions relative to the neocortex. White matter damage is common in human cases of small-vessel disease,[16] thus our model at least partially reflects the topographic distribution of lesions in patients. The severity of neuronal damage produced by micoinfarcts was greatest in the hippocampus, where we often observed cell death. This effect is reminiscent of the selective neuronal damage after global ischemia, however, there are also key differences to mention. First, neuronal damage in our model was found throughout all sectors of the Cornu Ammonis fields (not just CA1, as in global ischemia), as well as the dentate gyrus and hilus. Second, the form of ischemia is obviously different, as in our case

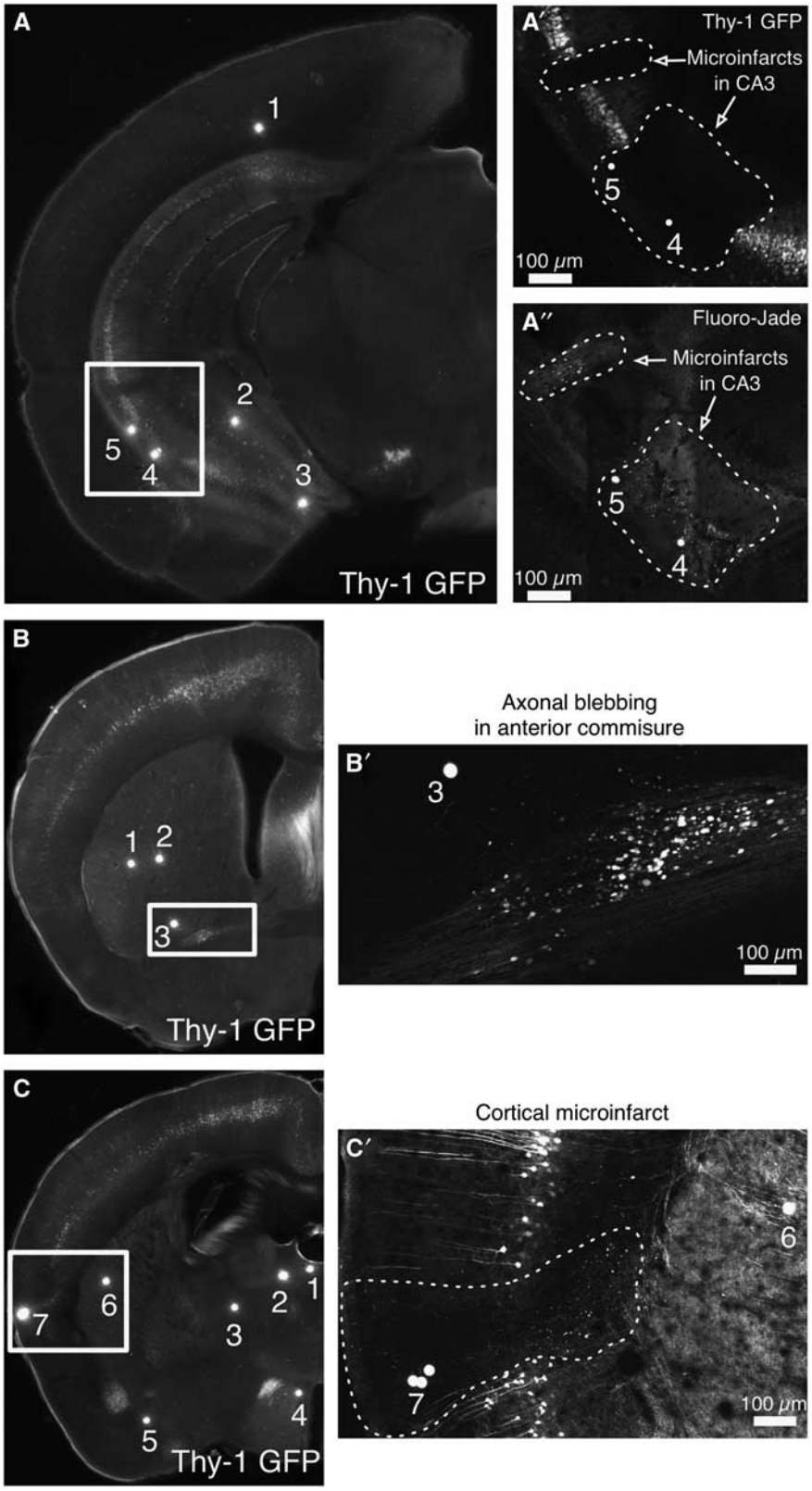

Figure 2. Example of hippocampal microinfarcts in a coronal section with microspheres lodged at multiple sites (1 to 5; **A**). Two microspheres (4 and 5) produced a focal loss of green fluorescent protein GFP-expressing cells (**A'**), and the presence of Fluoro-Jade-positive neurons within the same area (**A"**). The smaller infarct, also in the CA3 region was caused by a microsphere in an adjacent section (not shown). Microspheres near white matter tracts such as the anterior commissure (**B**) produced blebbing and loss of fiber structure (**B'**). Neocortical microinfarcts were relatively rare (**C**), but in severe cases were also characterized by a loss of GFP-expressing cells (**C'**).

the microspheres produce a permanent impairment in blood flow, while global ischemia is transient.

In sum, we show that endovascular injection of microspheres in mice may be used to study the regional distribution of microocclusions, and the neuronal atrophy that occurs focally throughout the brain. Although microinfarcts are known to accumulate over months and years in humans, endovascular aneurysm repair often produces an acute shower of microinfarcts.[17] Our simple and convenient method may be further combined with functional assessment tools such as longitudinal imaging of cortical activity or behavioral testing to assess potential therapeutic interventions.

DISCLOSURE/CONFLICT OF INTEREST

The authors declare no conflict of interest.

ACKNOWLEDGMENTS

The authors thank Victor Paraschiv, Sunny Wang, Pumin Wang, and Kenneth Chu for excellent technical assistance and preliminary work on this study. The authors also thank Drs Brian MacVicar and Louis-Philippe Bernier for providing the CX3CR1$^{GFP/+}$ mice.

REFERENCES

1 Smith EE, Schneider AJ, Wardlaw MJ, Greenberg MS. Cerebral microinfarcts: the invisible lesions. *Lancet Neurol* 2012; **11**: 272–282.
2 Cianchetti FA, Kim DH, Dimiduk S, Nishimura N, Schaffer CB. Stimulus-evoked calcium transients in somatosensory cortex are temporarily inhibited by a nearby microhemorrhage. *PLoS One* 2012; **8**: e65663.
3 Shih AY, Blinder P, Tsai PS, Friedman B, Stanley G, Lyden PD *et al.* The smallest stroke: occlusion of one penetrating vessel leads to infarction and a cognitive deficit. *Nat Neurosci* 2012; **16**: 55–63.
4 Rapp JH, Pan XM, Yu B, Swanson RA, Higashida RT, Simpson P *et al.* Cerebral ischemia and infarction from atheroemboli $<$ 100 microm in Size. *Stroke* 2003; **34**: 1976–1980.
5 Jiwa NS, Garrard P, Hainsworth AH. Experimental models of vascular dementia and vascular cognitive impairment: a systematic review. *J Neurochem* 2010; **115**: 814–828.
6 Wang M, Iliff JJ, Liao Y, Chen MJ, Shinseki MS, Venkataraman A *et al.* Cognitive deficits and delayed neuronal loss in a mouse model of multiple microinfarcts. *J Neurosci* 2012; **32**: 17948–17960.
7 Feng G, Mellor RH, Bernstein M, Keller-Peck C, Nguyen QT, Wallace M *et al.* Imaging neuronal subsets in transgenic mice expressing multiple spectral variants of GFP. *Neuron* 2000; **28**: 41–51.
8 Hall CN, Reynell C, Gesslein B, Hamilton NB, Mishra A, Sutherland BA *et al.* Capillary pericytes regulate cerebral blood flow in health and disease. *Nature* 2014; **508**: 55–60.
9 Enright LE, Zhang S, Murphy TH. Fine mapping of the spatial relationship between acute ischemia and dendritic structure indicates selective vulnerability of layer V neuron dendritic tufts within single neurons in vivo. *J Cereb Blood Flow Metab* 2007; **27**: 1185–1200.
10 Sozmen EG, Kolekar A, Havton LA, Carmichael ST. A white matter stroke model in the mouse: axonal damage, progenitor responses and MRI correlates. *J Neurosci Methods* 2009; **180**: 261–272.
11 Martina M, Brinckmann MP, Foddis M, Kunz A, Po C, Curato C *et al.* Vascular change and opposing effects of the angiotensin type 2 receptor in a mouse model of vascular cognitive impairment. *J Cereb Blood Flow Metab* 2014; doi:10.1038/jcbfm.2014.221.
12 Zhu L, Hoffmann A, Wintermark M, Pan X, Tu R, Rapp JH. Do microemboli reach the brain penetrating arteries? *J Surg Res* 2012; **176**: 679–683.
13 Silasi G, Murphy TH. Stroke and the connectome: how connectivity guides Therapeutic Intervention. *Neuron* 2014; **83**: 1354–1368.
14 Lam CK, Yoo T, Hiner B, Liu Z, Grutzendler J. Embolus extravasation is an alternative mechanism for cerebral microvascular recanalization. *Nature* 2010; **465**: 478–482.
15 Cavaglia M, Dombrowski SM, Drazba J, Vasanji A, Bokesch PM, Janigro D. Regional variation in brain capillary density and vascular response to ischemia. *Brain Res* 2001; **910**: 81–93.
16 Papma JM, de Groot M, de Koning I, Mattace-Raso FU, van der Lugt A, Vernooij MW *et al.* Cerebral small vessel disease affects white matter microstructure in mild cognitive impairment. *Hum Brain Mapp* 2014; **35**: 2836–2851.
17 Cronqvist M, Wirestam R, Ramgren B, Brandt L, Nilsson O, Säveland H *et al.* Diffusion and perfusion MRI in patients with ruptured and unruptured intracranial aneurysms treated by endovascular coiling: complications, procedural results, MR findings and clinical outcome. *Neuroradiology* 2005; **47**: 855–873.

Supplementary Information accompanies the paper on the Journal of Cerebral Blood Flow & Metabolism website (http://www.nature.com/jcbfm)